Journal of the Brazilian Society of Mechanical Sciences and Engineering (2022) 44:371
https://doi.org/10.1007/s40430-022-03689-3

TECHNICAL PAPER

Analysis of Ranque–Hilsch vortex tube cooling performance in respect of cutting temperature, resultant cutting force and chip morphology in turning of BeCu alloy

Ramazan Çakıroğlu[1]

Received: 10 March 2022 / Accepted: 13 July 2022
© The Author(s), under exclusive licence to The Brazilian Society of Mechanical Sciences and Engineering 2022

Abstract
Recently, it has been seen that environmentally friendly cutting media are widely used to contribute to sustainability in the processing of engineered materials. In this context, a study has been focused on both contributing to the mentioned purpose and turning a beryllium-copper (BeCu) alloy on which much research has not been done on its machinability despite being used in a wide industrial area. For this purpose, a comprehensive study was performed to determine the effects on the cutting temperature, resultant cutting force and chip morphology of the cutting speed, feed rate and depth of cut in the machining of C17500 alloy under dry and Ranque–Hilsch vortex tube (RHVT) cutting environments. Turning experiments were carried out with Al_2O_3 + TiCN-coated carbide tools, and the changes on the cutting tool were investigated by SEM and EDX analyses. The cutting temperature values revealed in the RHVT application were measured 62.6% lower on average compared to the dry cutting environment. The Fr values obtained for the RHVT cutting environment were on average 11.6% higher than those in the dry condition. The chip thickness ratio was obtained larger in the experiments performed in the RHVT application, and the most important secondary parameter affecting it is the depth of cut. In addition, more than 99% compatibility was found between the mathematical model predictions developed for the cutting temperature, the resultant cutting force and the actual test results.

Keywords Beryllium-copper · Ranque–Hilsch vortex tube · Cutting temperature · Cutting force · Chip morphology

1 Introduction

Today, studies are focused on improving the mechanical and physical properties of materials to meet the material demands in the fields of defense, nuclear, automotive, space and aviation. Hybrid materials have started to be produced to gain the desired properties to the materials. Beryllium-copper (BeCu) alloys are one of these hybrid materials [1]. These alloys, which have properties such as high strength and hardness, impressive thermal and electrical conductivity and excellent wear resistance, are widely used in the fields of defense, nuclear, aerospace, automotive, manufacturing, electrochemistry, medicine and marine [2–4]. On the other hand, while the newly developed materials gain superiority in terms of their mechanical and physical properties, many uncertainties and problems arise in the processing processes. For example, it is important to process the material without undergoing structural changes in order to achieve the desired performance, and at this point it becomes important to control the cutting zone temperature [5]. Furthermore, high cutting forces and raised temperature values during cutting negatively affect tool wear, tool life, workpiece surface quality and dimensional precision. To diminish these adverse effects, high amounts of cutting fluids are sprayed on the cutting area. However, the fact that cutting fluids used in traditional cooling methods are harmful to humans and the environment has led to the development of alternative cooling/lubrication methods [6].

In turning operation, the material being machined, cutting tool material and geometry and cooling/lubrication methods are the main factors affecting the machining performance and these are the determining factors in the selection of feed rate, cutting speed and depth of cut, which directly impact

Technical Editor: Izabel Fernanda Machado.

✉ Ramazan Çakıroğlu
rcakiroglu@gazi.edu.tr

[1] Vocational School of Technical Sciences, Gazi University, Ankara, Turkey

Published online: 30 July 2022

the machinability indicators. Increasing material quality, reducing processing costs and environmental damage for sustainable products have become a necessity in today's industry [2, 7, 8]. In this context, some of the recent studies on the turning of non-ferrous metals such as copper alloy, Ti and Ni alloy materials in various cutting/lubricating environments are summarized below. Alagarsamy et al. investigated the effects of machining parameters on material removal rate (MRR) and surface roughness (SR) with Taguchi-based gray relational analysis in the dry turning process of beryllium-copper (C17200) alloy. ANOVA result shows that cutting speed was the major factor on multiresponse characteristics followed by the depth of cut [2]. García-Martínez et al. performed a low initial lubrication condition on the cutting zone in the nanoscale machining of beryllium-copper [5]. Saikiran et al. conducted a study on the effects of vegetable oil-based cutting fluids in the machining of copper alloys. In their study, they determined the most ideal parameter by optimizing the results of cutting force intensity, MRR and superficial finishing [9]. Hong et al. reported that spraying liquid nitrogen (LN2) on the cutting zone was effective in reducing the temperature in the cutting zone [10]. By spraying a minimum amount of oil (MQL) on the cutting area, the machining performance is improved by reducing the temperature in the cutting area [11, 12]. To reduce the negative effects on the environment and human health in the MQL method, studies have been carried out on the use of various vegetable oils [13, 14]. However, as mentioned in some studies, the very small amount of liquid used in the MQL method cannot fully fulfill its cooling task due to sudden evaporation at high cutting zone temperatures [15, 16].

Cooling methods used in machining operations should neither reduce the temperature in the cutting zone so much that it makes chip removal difficult nor allow the formation of high cutting force and cutting zone temperature. For this reason, the cold air degree and pressure must be adjustable in the cooling processes applied to the cutting area. In recent years, Ranque–Hilsch vortex tube (RHVT) cooling has come to the fore both because of these advantages and because it is an easy to carry, low price and more significantly eco-friendly cooling system [17, 18]. Gases such as carbon dioxide, oxygen, nitrogen, air and water vapor are used in this system. Air and water vapor are in a more convenient position owing to their reduction in costs and eco-friendly than others [19, 20]. Applying cold air to the cutting zone with RHVT contributes to the reduction in cutting zone temperature, cutting forces, surface roughness, increasing tool life and reducing cutting costs [21–25]. Çakıroğlu investigated the impact of cutting parameters on surface roughness, main cutting force and cutting zone temperature under different cooling conditions (Dry, MQL and vortex tube) to improve the machinability performance of Inconel718 material with Taguchi-based gray relational analysis [18]. Mia et al. examined the consequences of vortex tube and nitrogen gas-assisted MQL on surface roughness (Ra) and tool wear in the turning of Al 6061-T6 alloy [26]. Kumar et al. compared vortex tube application with dry, wet and MQL cutting environments during hard turning of AISI 4340 steel. They determined that the cold air produced by the vortex tube has a seriously positive effect on tool wear, cutting force and surface roughness [27]. Günay et al. analyzed the cutting tool life and wear mechanisms and the machined surface in the turning of Nimonic 80A superalloy in different machining environments such as dry, air cooling and oil spraying method [28].

The literature review shows that investigations have been executed on the analysis of machinability indicators such as tool wear, cutting force, surface roughness in different cutting/lubricating fluid environments such as dry, air, or gas cooling and MQL with various vegetable oil content in the machining of non-ferrous materials. Although the RHVT cooling system is both low cost and provides a sustainable cutting environment, it has been found that it is not used in the machining of BeCu alloys. In addition, no studies were found for the mentioned material on measuring the cutting temperature, which is one of the most active factors on tool wear and/or modeling any machinability indicators. In this context, it is very obvious that a detailed analysis of RHVT cooling performance on cutting force, cutting zone temperature and chip morphology in the machining of BeCu alloy using variable cutting speed, depth of cut and feed rate will contribute to the deficiency in the literature. In this study, firstly, cutting forces and cutting temperature were measured during the turning of C17500 BeCu alloy with coated carbide tool in dry and RHVT cutting environments. Then, predictive models were developed by regression analysis for the calculated resultant force and the measured cutting zone temperature. The results of the research will contribute to the selection of optimal cutting parameters in the machining of BeCu alloy in a cheap and environmentally friendly cutting environment and indirectly to increase the machining efficiency in the related industries.

2 Material and method

2.1 Material, equipment and experimental strategy

In the turning experiments, cylindrical beryllium-copper (BeCu) C17500 alloy with dimensions of Ø40X300 mm was used as the workpiece material. This material, whose mechanical and physical properties are improved by precipitation hardening and aging heat treatments after being shaped by hot forging, is used in places that require high hardness, electrical and thermal conductivity. BeCu alloys are used in many products such as electrical/electronic

connectors, current carrying springs, precision screw machined parts, welding electrodes, bearings, plastic molds and aircraft landing gear bushings. On the other hand, the hard structure of Be particles in BeCu alloys can cause adverse effects on the cutting tool [1, 2]. Therefore, it is important to investigate the machinability of this material according to different cutting environments and cutting parameters. The chemical composition and properties of the BeCu alloy are given in Table 1. The experiments were carried out on the Johnford TC35 industrial type CNC lathe, which can operate at 10 KW power and a maximum speed of 3500 rpm. To obtain data that are more reliable by providing a more rigid cutting process, the processing was done between the chuck and the tailstock.

Sumitomo brand WNMG 080404 geometry and AC610M quality CVD (Al_2O_3 + TiCN) carbide-coated tools were used in the machining of BeCu alloy. The insert is made resistant to wear and chip adhesion with an ultra-hard micro-grain coating (5µ). CVD-coated tips are widely used to examine flank wear, crater wear, nose deformation, built-up edge formation, etc. [29, 30]. Coated carbide tool has been used, especially in ductile materials, since the adhesion mechanism is common in uncoated tools. DWLN R/L 2020K08 holder with a 95° approach angle is used as a tool holder. Two different cutting environments (dry and vortex tube cooling) and three different levels of cutting speed, feed rate and depth of cut were used in the experiments. In the stage of determining the levels of the cutting parameters, researches on the machining of Be-Cu alloys and cutting tool catalog information were used. According to the cutting parameters given in Table 2, 27 experiments were performed separately in dry and RHVT cutting conditions. The assessments were made by taking the average of the measured cutting forces and temperatures from the two repeated experiments.

In the second part of the experiments, a vortex tube cooling system called Ranque–Hilsch vortex tube (RHVT) was used. The RHVT has control valve components where there is an air inlet, hot and cold air outlet and hot air outlet [31]. The working principle of RHVT is given in Fig. 1. Before starting the experiments, the air coming from the compressor was transferred to the system using the inlet nozzle of the vortex tube and the pressure value in the system was checked with a monometer. The pressure adjustment process was made with the pressure regulator and the cold air value with the control valve at the hot air outlet. In the experiments, cold air was sent to the tip of the cutting tool at −2 °C at 4.5 bar pressure. A digital thermometer with a precision of ± 0.5 °C controlled the cold air temperature at the tooltip. The outlet nozzle of the cold air was set at a distance of 5 mm from the cutting tool tip in all experiments.

FLIR T440 type thermal camera was used to measure the temperature values released during the cutting process. The thermal camera can measure between 0 and 1200 °C and measurements were taken at a distance of 25 cm from the tool tip. The most important parameter in measurements with a thermal camera is the emissivity (Ɛ) value. In this study, the temperature measurement system was set and calibrated at Ɛ = 0.04. The calibration process was checked by comparing the measurement result of the surface temperature of the BeCu alloy, which was kept at room temperature for 24 h, with a digital thermometer with a sensitivity of ± 0.01 °C. For each test condition, the highest temperature value creating along the cutting length (25 mm) was used in the evaluations of cutting temperature. KISTLER 9257A type piezoelectric dynamometer was used for force measurements during the cutting process. This dynamometer was connected to a KISTLER Type 5019 signal amplifier (Multichannel Charge Amplifier), and the cutting forces were sent to the computer with an RS-232C patch cable and raw graphs of the force components were obtained with the DynoWare Type 2825A-2 program. Analyses were made by taking the average of the force components measured along the cutting length.

Table 2 Cutting parameters and their levels

Parameters	Unit	Symbol	Level 1	Level 2	Level 3
Cooling condition	–	CC	Dry	RHVT	–
Cutting speed	m/min	Vc	150	180	210
Feed rate	mm/rev	*f*	0.06	0.08	0.1
Depth of cut	mm	ap	0.5	0.75	1

Table 1 Chemical composition and properties of the BeCu (C17500) alloy

Chemical composition of BeCu (C17500) alloy					
Elements	Co	Ni	Be	Cu	–
Weight (%)	2.5	0.3	0.5	Remaining	–
Properties of BeCu (C17500) alloy					
Density (g/cm^3)	Rockwell Hardness (HrB)	Yield strength (N/mm^2)	Tensile strength (N/mm^2)	Electric conductivity (MS/m)	Thermal conductivity (W/mK)
8.8	100	500–600	700–800	24–30	230

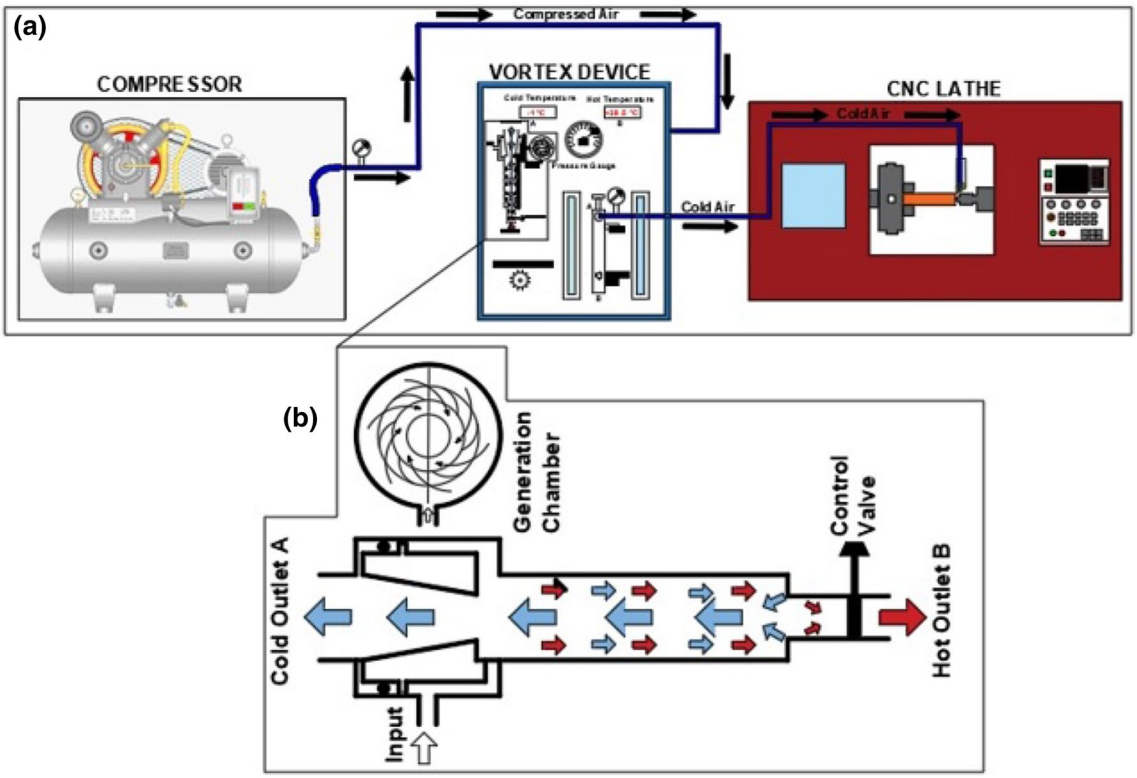

Fig. 1 **a** Application of the RHVT system in turning, **b** RHVT working principle

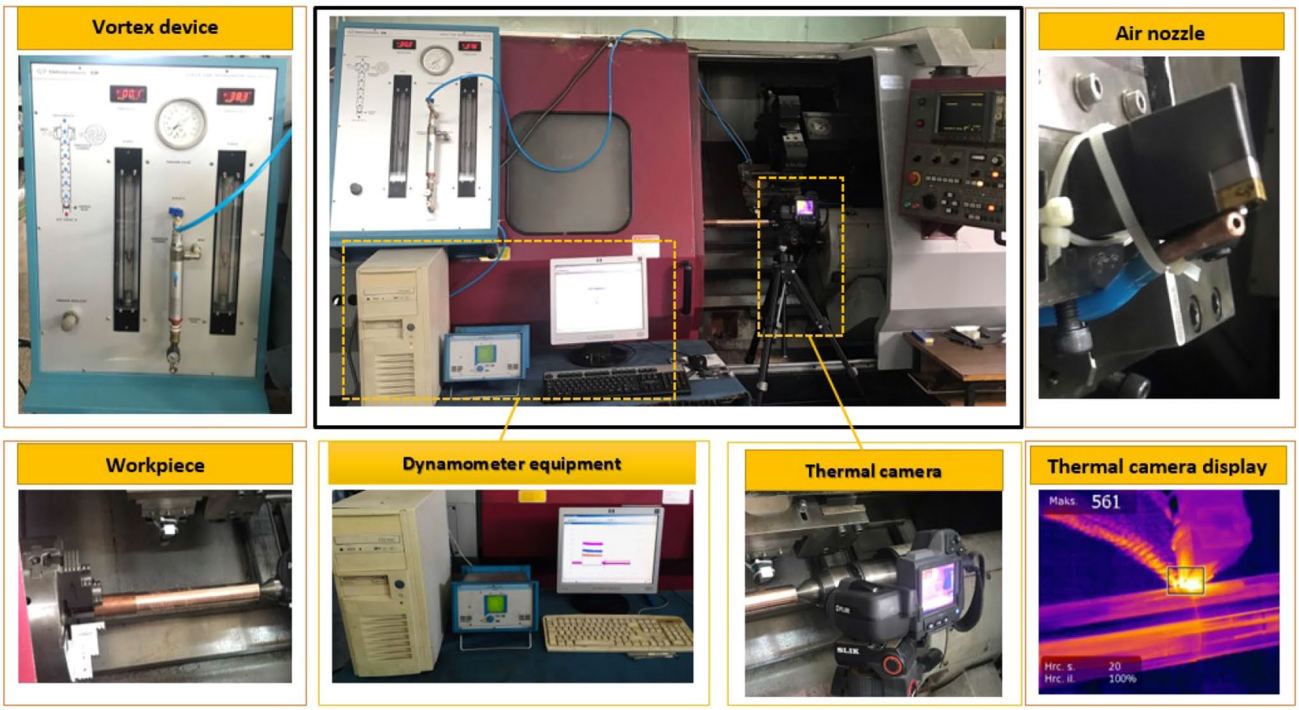

Fig. 2 Stages of the experimental study

Cutting forces have three components, which are in the *x*-axis (Ff), *y*-axis (Fp) and *z*-axis (Fc), as shown in Fig. 2. The resultant cutting force (Fr) is calculated from the combination of these forces, and the Fr is evaluated in this study. Scanning electron microscopy (SEM) and EDX analyses were performed to determine the wear mechanisms and types of cutting tools after the experiments.

In the last stage of the study, a detailed analysis of the chip types was made in the turning of BeCu alloy in different cutting environments. For this purpose, the chip collected after each experiment was placed in ziplock bags to prevent oxidation. Chip thickness was measured for each test to find the chip thickness ratio (CTR), which is an important machinability index. CTR values were calculated as the ratio of uncut chip thickness to chip thickness. Measurements were made using an electronic digital caliper manufactured by Mitutoyo with a precision of ± 0.01 mm. CTR values were evaluated by calculating the average of three measurements made from a chip. The steps of the experimental study and the details of the equipment used are given in Fig. 2.

3 Results and assessment

In this study, cutting temperature (T) and resultant cutting force (Fr) values obtained in machining of C17500 alloy under dry and vortex tube cooling environments in order to contribute to environmentally friendly and sustainable production are given in Table 3.

3.1 Cutting zone temperature

Depending on the cutting environment and cutting parameters, the high-temperature value in the cutting zone has negative effects on the workpiece and cutting tool, such as surface integrity, dimensional accuracy and tool life [32]. It is very important to keep the temperature formed in the cutting zone under control in order to reduce these negativities to minimum levels [18]. Therefore, the effect of RHVT application on the cutting zone temperature according to dry cutting conditions was compared experimentally. The cutting zone temperature changes obtained in turning of

Table 3 Experimental design and experimental results

Exp. no	Vc (m/min)	*f* (mm/rev)	ap (mm)	T-Dry (°C)	T-Vortex (°C)	Fr-Dry (N)	Fr-Vortex (N)
1	150	0.06	0.5	464	409	549	637
2*	150	0.08	0.5	452	352	620	692
3	150	0.1	0.5	451	329	606	670
4	150	0.06	0.75	486	308	631	716
5	150	0.08	0.75	461	247	666	761
6	150	0.1	0.75	435	231	643	688
7	150	0.06	1	515	268	696	807
8*	150	0.08	1	473	249	568	654
9	150	0.1	1	452	216	605	674
10*	180	0.06	0.5	523	490	613	703
11	180	0.08	0.5	482	453	642	739
12	180	0.1	0.5	458	401	620	664
13*	180	0.06	0.75	547	313	642	730
14	180	0.08	0.75	529	268	518	618
15	180	0.1	0.75	510	246	551	631
16	180	0.06	1	562	281	561	641
17	180	0.08	1	544	257	605	681
18*	180	0.1	1	518	232	596	651
19	210	0.06	0.5	574	545	621	691
20	210	0.08	0.5	536	464	658	731
21*	210	0.1	0.5	502	412	588	677
22	210	0.06	0.75	582	325	667	768
23	210	0.08	0.75	561	282	537	630
24*	210	0.1	0.75	526	263	585	655
25	210	0.06	1	596	295	672	766
26	210	0.08	1	570	271	585	664
27	210	0.1	1	537	258	629	715

*Experiments hidden in regression analysis

C17500 alloy according to the cutting conditions presented in Table 2 are given in Figs. 3 and 4. In general, the cutting zone temperature measured in the RHVT cutting environment was lower than the machining performed in dry conditions for all experiments.

In the dry cutting environment, it is seen that the cutting temperature decreases with increasing feed rate for all cutting speeds (Fig. 3). This indicates the inverse effect of the feed rate on the cutting temperature when the cutting speed is constant. This result can be explained about the distribution and removal of the heat generated in the cutting zone. For low feed rate values, the temperature of the tool–chip interface increases as the cutting tool will be in contact with the workpiece for a longer time, similarly Ref. [33]. In addition, the increase in the coefficient of friction at low feed rates results in more heat generation [34]. Because of these formations, the rise in the feed from 0.06 to 0.1 mm/rev decreased the cutting zone temperature. However, the interaction of higher cutting speed and feed rates and shortening of the cutting time reduced the temperature produced by the cutting process. At the same time, it is seen that there is a fluctuating change in cutting temperature with increasing depth of cut and it can be said that these changes are not significant. Increasing the depth of cut from 0.5 to 1 mm caused a change of about 7% in the cutting zone temperature. However, the increase in chip thickness with increasing feed and depth of cut contributed to the removal of more heat from the environment and thus to a decrease in the cutting zone temperature (Fig. 3). The highest cutting zone temperature was measured as 596 °C at $Vc = 210$ m/min, $f = 0.06$ mm/rev, $ap = 1$ mm experiment array in the dry cutting environment.

Cutting temperatures obtained in cutting processes with RHVT showed little increase with increasing cutting speed. On the other hand, increasing feed rate and depth of cut decreased the cutting zone temperature (Fig. 4). The lowest cutting temperature obtained under dry cutting conditions and the lowest cutting temperature obtained using RHVT were 435 °C and 216 °C, respectively. In other words, the use of RHVT reduced the cutting zone temperature by approximately 50%. The reason for this decrease can be attributed to the contribution of cold air sprayed to the cutting zone with high pressure to the rapid removal of chips in the cutting zone. Because most of the heat generated in the cutting zone is removed from the cutting zone by chips [35]. In addition, the correct positioning of the cold air nozzle directly affects the RHVT performance [36]. This study clearly shows that RHVT is very safe in terms of environment and worker health in the manufacturing industry and

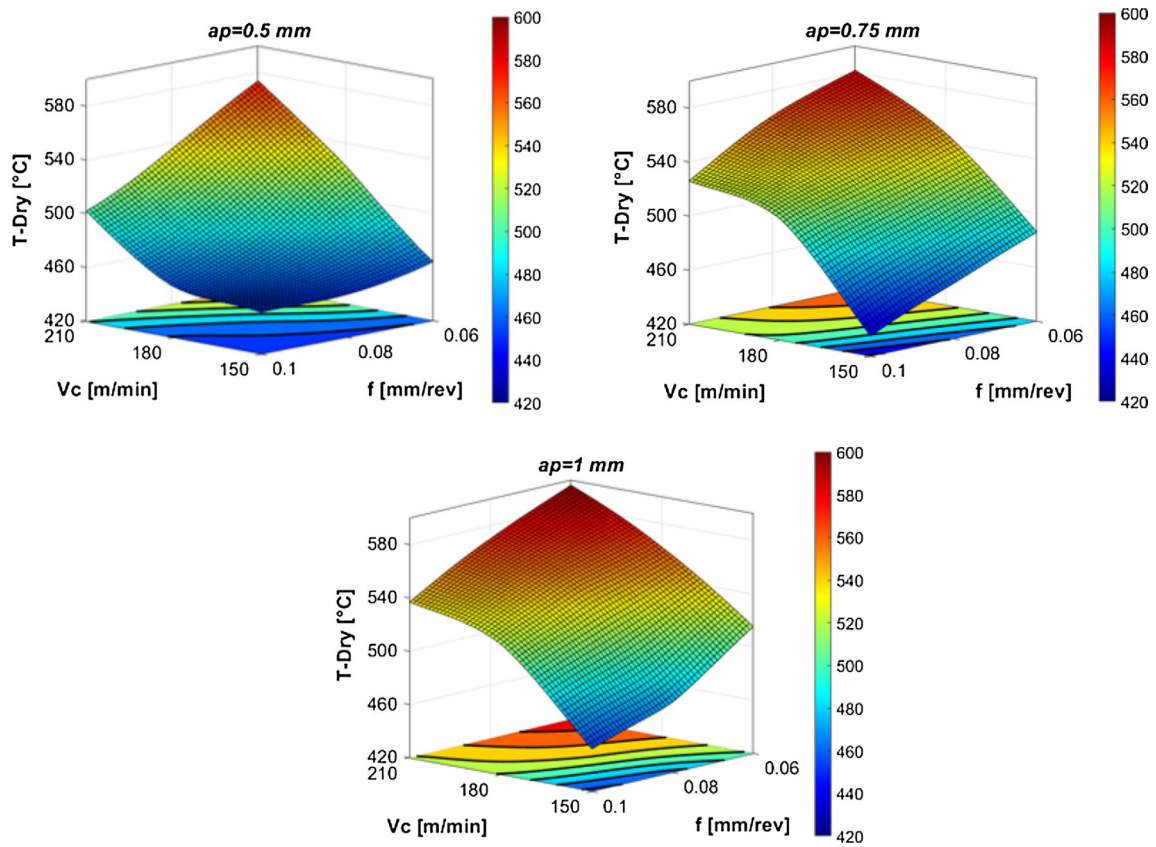

Fig. 3 Interaction graphics of T for dry condition

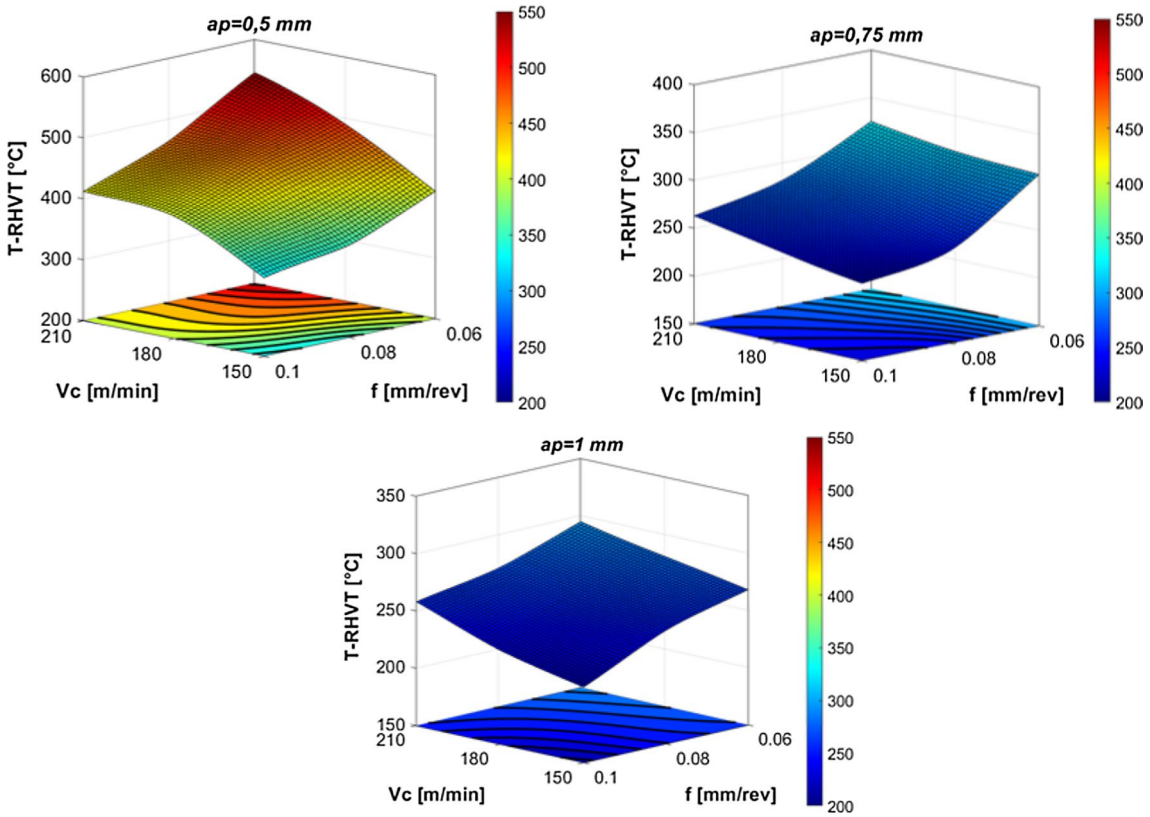

Fig. 4 Interaction graphics of T for RHVT condition

also very effective in reducing the cutting zone temperature in machining of BeCu alloy.

3.2 Cutting force

In addition to cutting conditions and cutting parameters, cutting forces are closely associated with the material properties to be machined and the properties of the cutting tool. Another aim of this study is to find the cutting parameters that will minimize the cutting forces in turning of BeCu alloy under dry and RHVT conditions. On the other hand, the force components that occur during turning operations, namely main cutting force (Fc), feed force (Ff) and the passive force (Fp), are used to calculate or estimate the power required to remove chips. At the same time, it is more meaningful to evaluate the resultant force (Fr) instead of these forces, which are responsible for energy consumption together. In this regard, the Fr values were calculated and analyzed using the equation given in Ref. [37].

The changes in the Fr values obtained in the turning of the BeCu alloy in the dry cutting environment according to the cutting parameters are given in the graph in Fig. 5. When Fig. 5a is examined, it is seen that the Fr force decreases with increasing cutting speed. This decrease in Fr force was mainly caused by the increase in temperature in the cutting zone with increasing cutting speed. Usually, the temperature in the cutting zone increase with cutting speed. That is, increasing temperature in the cutting zone decreased the yield strength of the workpiece and reduced the power required for chip formation [38]. On the other hand, it is seen that the Fr force increases significantly with the increase in depth of cut (Fig. 5). Since the depth of cut is one of the two components that make up the chip section ($ap * f$), it is expected that Fr will increase with its increase. When the depth of cut is increased from 0.5 mm to 1 mm, the Fr values increased by an average of 14.23% for the 150 m/min cutting speed, 13.23% for the 180 m/min cutting speed and 13.45% for the 210 m/min cutting speed. On the other hand, while the depth of cut is constant, an average of 10.19–11.82% increases in Fr values occurred at three cutting speeds with the increase in feed. From this, it can be said that the depth of cut has a more pronounced effect on the cutting forces. In the dry machining condition, the lowest Fr force was measured as 518 N in machining with the experiment array $Vc = 210$ m/min, $f = 0.06$ mm/rev, $ap = 0.5$ mm.

The changes in the Fr values obtained in the RHVT application according to the interaction of the cutting parameters are presented in the graphics in Fig. 6. When the graphics are examined in general, the Fr values are higher than the results in the dry cutting environment. A similar result was

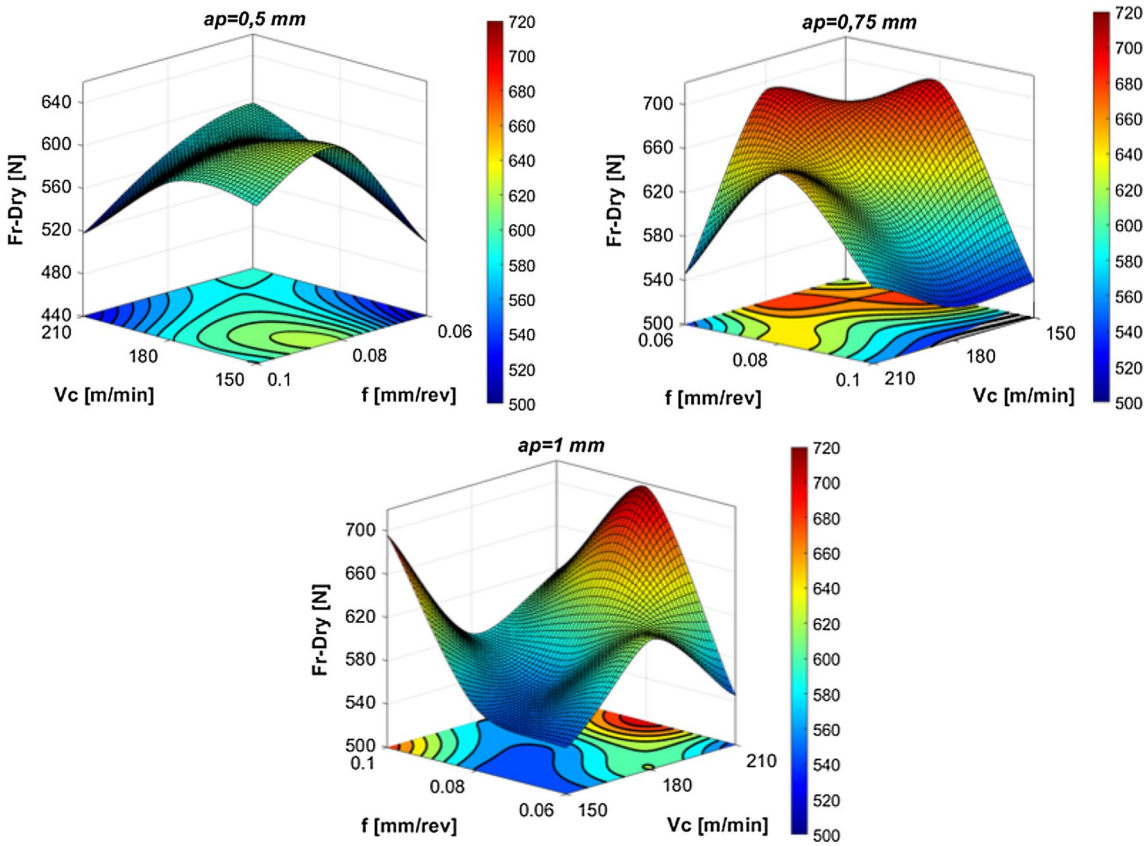

Fig. 5 Interaction graphics of Fr for dry condition

obtained by Hu et al. [22] during machining of steel material. This situation can be attributed to the formation of chips due to the rapid solidification of the machining area by the air sprayed at low temperature to the cutting area. When the cold air is sprayed on the cutting area, the friction force will be higher due to the lack of lubrication effect and the loads acting on the tool in the secondary deformation zone have enlarged and the resultant force has increased. In the case of RHVT, the highest Fr value was calculated as 806.6 N in the series of experiments $Vc = 150$ m/min, $f = 0.1$ mm/rev and $ap = 1$ mm. The high Fr force in the stated experiment condition can be partially attributed to the fact that the cooling application creates a mechanism that prevents the shear strength of the material from decreasing, as mentioned in Ref. [36]. In this cutting condition, the lowest temperature of the cutting zone (216 °C) proves the accuracy of the mentioned phenomenon. On the other hand, it is possible to show the changes in the cutting tool geometry during cutting as another reason for the formation of larger Fr's in the RHVT cutting environment. In this context, SEM images were taken to observe the changes on the cutting tools. In addition, possible material adhesions on the tool during machining operations were determined by EDX analysis. Figures 7, 8, 9 and 10 show that wear types such as flank wear, nose wear, notch wear, crater wear do not occur in CVD ($Al_2O_3 + TiCN$) carbide-coated cutting tools. However, adhesion wear mechanisms such as built-up edge (BUE) and/or the built-up layer (BUL) were observed at the tip and edge of the tool. The existence of these mechanisms occurring on the cutting tool has been proved by EDX analysis. In particular, BUL/BUE formations in the finishing operation processes evaluate these wear mechanisms important, as they directly affect the workpiece dimensional accuracy and surface quality.

BUL and BUE formations can exhibit static or dynamic characteristics depending on the cutting parameters as well as the workpiece and cutting tool material properties. These formations on the cutting tool affect the machining performances by changing the initial geometry and friction behavior of the cutting tool [39, 40]. Considering these effects, the density differences of these mechanisms that occur on the cutting tool according to the machining conditions come to the fore. In Fig. 7, SEM images of tools used in dry and RHVT cutting environment at low cutting speeds, medium depth of cut and feed rate are given. As can be seen from the figure, the intensity of adhesion effects is striking in the tool cutting under the RHVT condition and BUE formations are observed on the main and auxiliary cutting edge of the tool

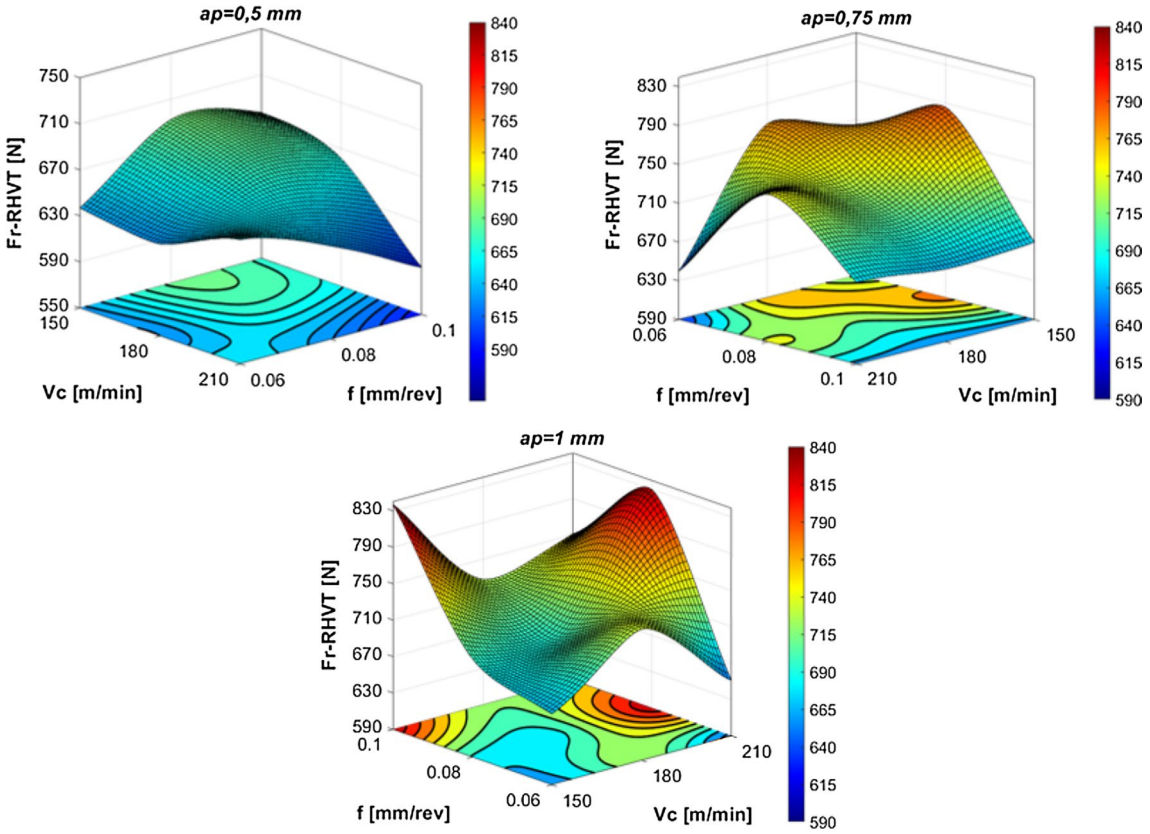

Fig. 6 Interaction graphics of Fr for RHVT condition

and BUL on the side surfaces. This was due to the fact that the RHVT application reduced the cutting zone temperature with the effect of pressure cooling instead of lubrication and increased friction forces in the second deformation zone. As shown in Fig. 8, it is seen that these mechanisms decrease a little due to the increasing cutting temperature with the increase in cutting speed [41, 42] and this has resulted in a slight decrease in cutting forces (Fig. 6). This result was confirmed by EDS analyses from tool and BUE/BUL from regions 1 and 2, respectively (Figs. 7, 8). When the EDS spectra are examined, it is seen that Cu peaks are intense in BUE/BUL formations and Al peaks are intense in the tool. However, the increase in the auxiliary cutting edge and the side surface of these mechanisms during machining caused an increase in the cutting tool radius. This increased the effect of the third deformation zone in the chip formation process. At the same time, the tool–workpiece contact area increased as the depth of cut increased, resulting in a decrease in the RHVT effect, and thus, the decreasing cutting zone temperature indirectly increased the BUL/BUE. This formation is clearly visible in Fig. 9. As a result, the resultant forces obtained in the RHVT cutting environment were high. On the other hand, when the depth of cut is increased from 0.5 to 1 mm, an increase in Fr values is inevitable as in dry cutting. The reason for this is attributed to the chip cross-section increasing with increasing *ap* value. As a result, the increase in Fr values for cutting speeds of 150, 180 and 210 m/min at constant depth of cut was on average 12.71%, 10.15% and 8.30%, respectively.

3.3 Chip morphology

Chip morphology plays a crucial role in decisive the machinability of non-ferrous metal alloys. At the same time, the chip morphology prominently affects the machined surface morphology and also the tool life owing to the mechanical–thermal behavior at the workpiece–tool interface. In this sense, understanding the chip formation mechanism of BeCu alloy in different cutting environments is important for machining efficiency.

An increase in the CTR value means a decrease in chip thickness, according to the equation (uncut chip thickness/chip thickness) used in its calculation. On the other hand, it means an increase in the chip compression ratio (1/CTR), which results in a higher friction force at the tool–chip interface [43]. The changes in the chip thickness ratio (CTR) values obtained in the dry and RHVT cutting environments are presented in Fig. 10. It is seen from the figure that CTR

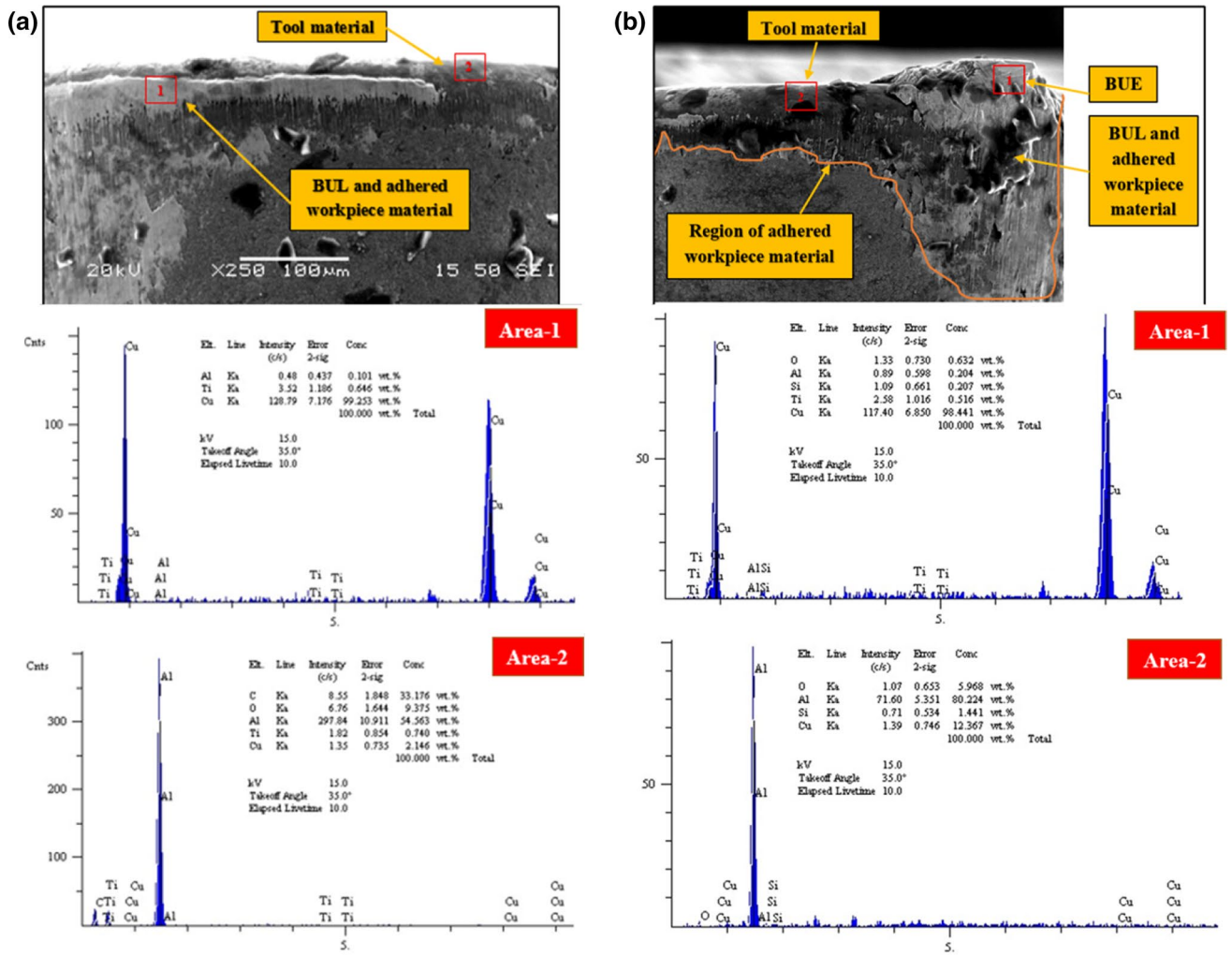

Fig. 7 SEM and EDX analysis at $Vc = 150$ m/min, $f = 0.06$ mm/rev, $ap = 0.75$ mm; **a** dry, **b** RHVT

values are higher in a dry application, while the CTR values increased with the increase in *Vc, f* and *ap* in both cutting environments. Thicker chips are produced during machining due to the increased chip cross-sectional area with increasing *ap* and *f*. At a cutting speed of 150 m/min, the CTR values increased by an average of 16.3% and 16.75% for dry and RHVT, respectively, as the feed increased from 0.06 to 0.1 mm/rev. While this ratio was 14.4% and 15.27% for $V = 180$ m/min, it was calculated as 11.62% and 12.64% for $V = 210$ m/min. From this, it can be said that the CTR changes significantly with the increase in cutting speed. Holding feed constant, CTR values increased on average 19.4% and 20.15% for dry and RHVT, respectively, with increasing depth of cut from 0.5 to 1 mm. While this ratio was 19.45% and 20.01% for $V = 180$ m/min, it was 24.61% and 24.32% for $V = 210$ m/min. As can be seen from the ANOVA given in Table 4, cutting speed is of primary importance and depth of cut is of secondary importance in increasing CTR.

That is, the increase in *f* and *ap* contributes to the proportional decrease in CTR. Thus, as the chip segment height and knurled increase, the chips show shorter and connected curve morphology (Fig. 11), as mentioned in Ref. [44]. It is also realized that the chips have a reddish-brown appearance. This change in chip color is more clearly seen in the experiments performed in the RHVT environment where the chip cross section increases (Fig. 11). At a higher *Vc*, the chip material softens too much due to the increased temperature, and as a result, the chip shear rate increases [45]. Then, chip segments are formed at smaller heights, resulting in smaller chip thickness due to the low friction at the tool–chip interface. Therefore, CTR values increase with increasing *Vc* and the pressure created by the friction effect in the second deformation zone decreases, helping to decrease the cutting forces. In other words, because the chips are thin, they move faster along the tool rake face and therefore show a larger curve radius and continuous chip type (Fig. 11). This phenomenon is valid for the machining of Be-Cu alloy in a

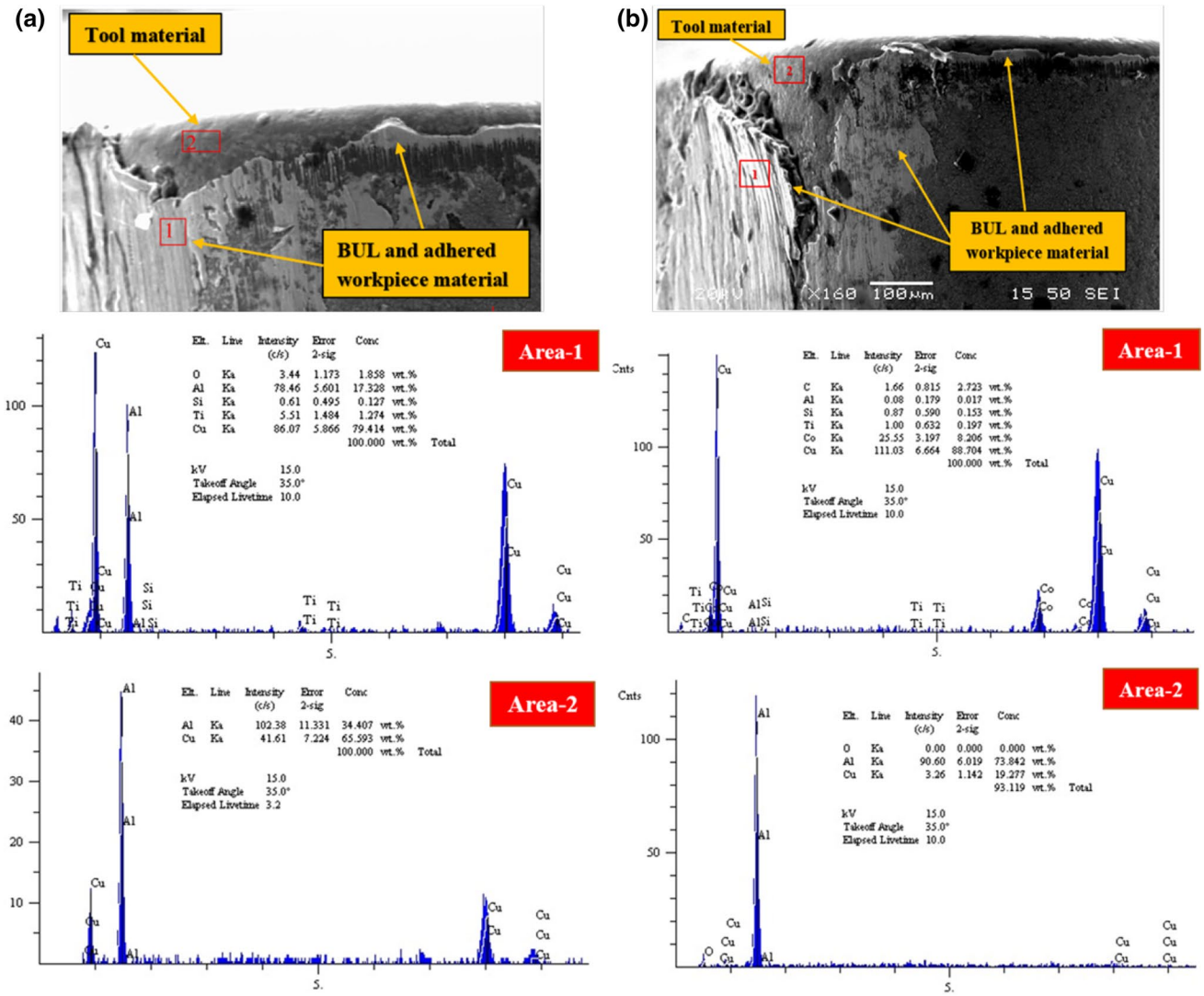

Fig. 8 SEM and EDX analysis at $Vc = 210$ m/min, $f = 0.06$ mm/rev, $ap = 0.75$ mm; **a** dry, **b** RHVT

dry environment, and as stated in Sect. 3.2, it both positively affected the formation of BUE and caused the cutting forces to be lower than RHVT. However, since the effect of compressed cold air reduces the cutting temperature in RHVT application, BUL/BUE formation occurred more with the decrease in chip shear rate. The thickness of the material adhesion will affect the chip flow rigidity, which has a negative effect on the force and temperature values. In addition, the lower cutting zone temperatures compared to the dry cutting environment made plastic deformation difficult and these formations caused an increase in chip thickness. As indicated by Tamizharasan et. al., this causes knurled chips and linked arc morphology especially at high *ap* and low *Vc* [46]. As a result, increased chip compression ratio resulted in higher cutting forces in RHVT application.

Additionally, deciding the effect levels of cutting parameters on the CTR contributes to the prediction of chip morphology and thus to improvement in basic machinability outputs for instance cutting force, surface quality, tool life. In this context, the results of the analysis of variance applied for CTR are given in Table 4. Here, the degree of freedom (DoF), the sum of squares (SS), mean squares (MS), F values and percentage contribution ratio (PCR) of every parameter are shown. Analysis of variance (ANOVA) and F test were performed to prove the significance of each factor. This analysis was carried out for a significance level of $\alpha = 0.05$ (confidence level of 95%). If a factor's P-value exceeds 0.05, that factor's contribution is statistically insignificant [47, 48]. By the ANOVA results, it was decided that the most prominent parameter on CTR for dry and RHVT machining was cutting speed with PCR of 55.61% and 56.43%, respectively. A secondary important parameter is cutting depth with PCR of 28.81% and 27.97%, respectively. From this, it was

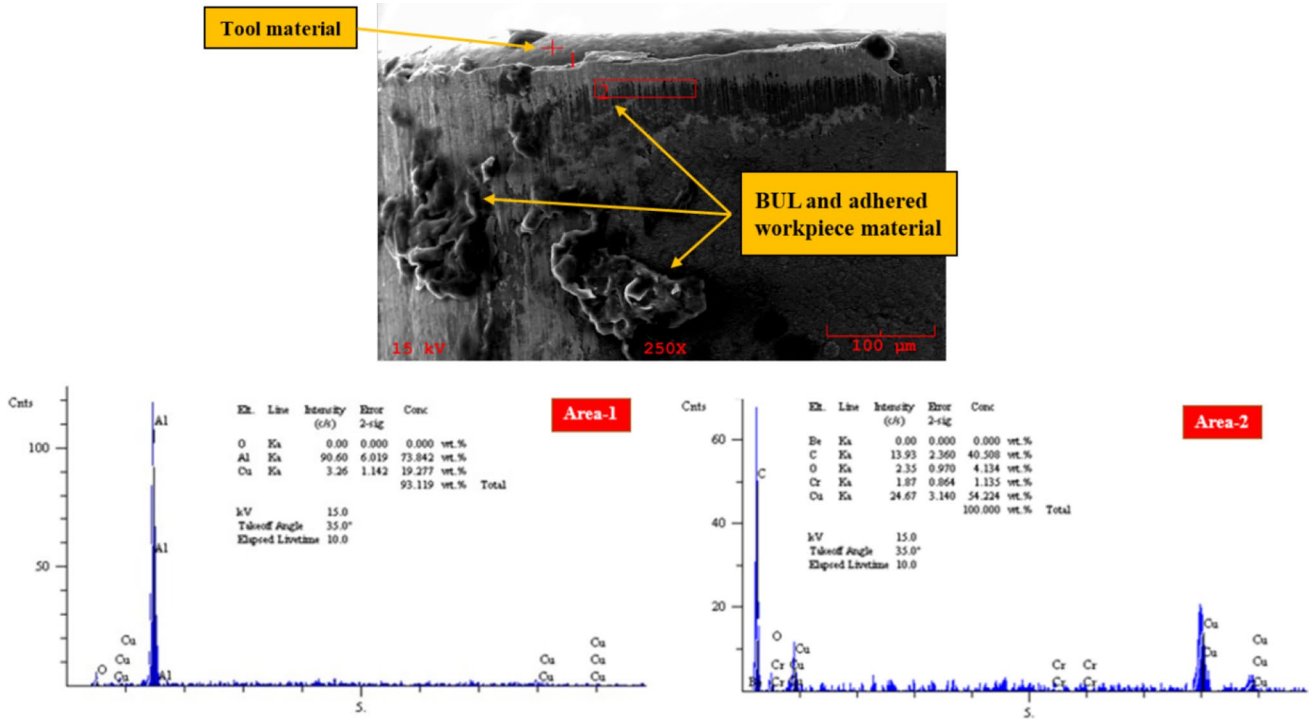

Fig. 9 SEM images at $Vc = 210$ m/min, $f = 0.06$ mm/rev, $ap = 1$ mm

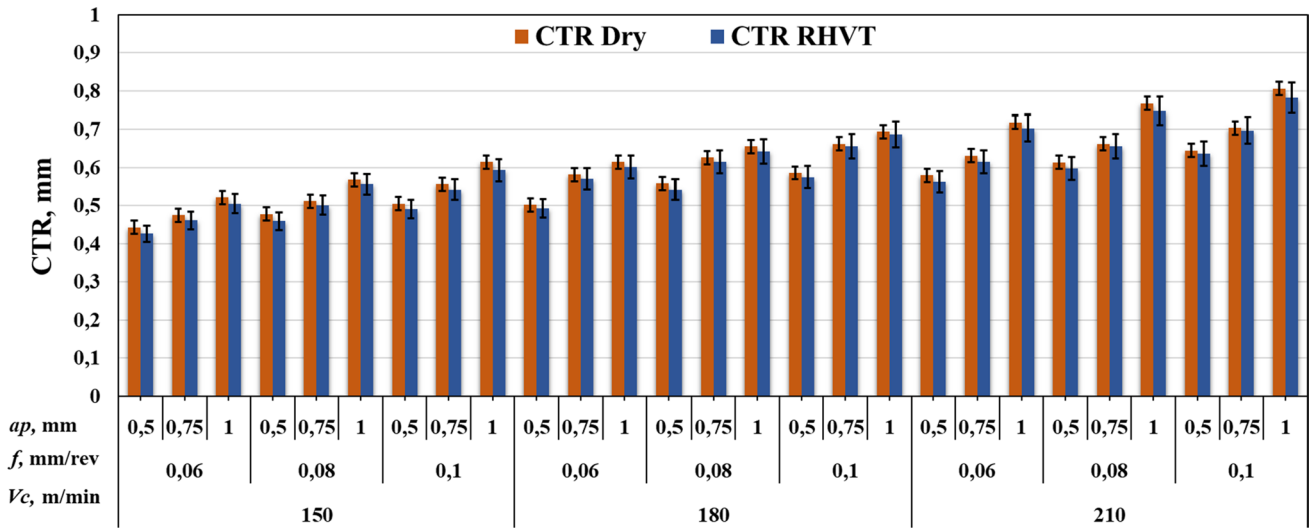

Fig. 10 CTR variations depending on cutting conditions

revealed that *ap* and *Vc* are premier parameters in terms of chip morphology.

3.4 Mathematical modeling of T and Fr

Mathematical modeling is used to predict an output variable or response based on numerous input variables in any field. Regression analysis is a widely used way to understand and improve the interaction between the output and the input variables. Each value of the independent variable is associated with the dependent variable. In Eq. 1, an example of a regression model with more than one variable is given [49].

$$y = \beta_0 + \beta_1 x_1 + \beta_2 x_2 + \cdots + \beta_n x_n + e \quad (1)$$

Table 4 ANOVA results for CTR

Parameter	DoF	SS	MS	*F*	*P*	PCR (%)
CTR-Dry						
Vc	2	0.118081	0.05904	217.5	0.000	55.61
f	2	0.027641	0.01382	50.91	0.000	13.02
ap	2	0.061182	0.030591	112.69	0.000	28.81
Error	20	0.005429	0.000271			2.56
Total	26	0.212332				100
CTR-RHVT						
Vc	2	0.120086	0.060043	290.91	0.000	56.43
f	2	0.029069	0.014534	70.42	0.000	13.66
ap	2	0.059526	0.029763	144.2	0.000	27.97
Error	20	0.004128	0.000206			1.94
Total	26	0.212809				100

Here y is the output variable, x is the input variable, β_0 is the intersection point, $\beta_{(1\text{-}n)}$ is the coefficients of the variables, e is the remaining error.

In this part of the study, the relationship between *Vc, f* and *ap* (input variables) of T and Fr results (output variables) obtained in dry and RHVT cutting environments was analyzed. In the evaluation, 20 test results randomly selected from 27 real experimental results of T and Fr were used for training while 7 test results were reserved for checking the correctness of the regression equation. The mathematical model for each T and Fr was developed using the full quadratic regression model by the Minitab 17 software. Predictive models for the cutting zone temperature and resultant cutting force are given in Eqs. 2–5. In these models, f is the feed rate in mm/rev, *Vc is* the cutting speed in m/min and a_p is the depth of cut in mm.

$$T_{(\text{Dry})} = -129 + 4.93 * v_c + 275 * f + 227 * a_p - 7 * v_c * f - 0.062 * v_c * a_p - 643 * f * a_p - 0.00788 * v_c^2 + 1196 * f^2 - 62 * a_p^2 \quad (2)$$

$$T_{(\text{RHVT})} = 810 + 5.81 * v_c - 7623 * f - 1715 * a_p 2.6 * v_c * f - 2.616 * v_c * a_p + 2475 * f * a_p - 0.0085 * v_c^2 + 22888 * f^2 + 1093 * a_p^2 \quad (3)$$

$$F_{r(\text{Dry})} = 467.1 - 1.695 * v_c + 901 * f + 512.2 * a_p + 4.05 * v_c * f - 0.481 * v_c * a_p + 942 * f * a_p + 0.00318 * v_c^2 + 4339 * f^2 - 130.1 * a_p^2 \quad (4)$$

$$F_{r(\text{RHVT})} = 126.6 + 2.93 * v_c - 3293 * f - 318.9 * a_p - 13.83 * v_c * f - 0.757 * v_c * a_p + 3111 * f * a_p - 0.00553 * v_c^2 - 8144 * f^2 + 193.2 * a_p^2 \quad (5)$$

Since predictive modeling with the regression method is carried out in two stages, training and testing, statistical analysis was conducted to determine the amount of deviation (error) between the predicted value and the actual value and the accuracy of the methods was checked. In this statistical analysis, determination coefficient (R^2), amount of statistical error (RMSE) and mean percent error (MAPE) were evaluated. The high values of R^2 and the lowest values of RMS and MAPE are the values for which the model has the highest performance [50]. These values were determined with the help of the following equations. Here, t is the target value, o is the output value, and N is the number of experiments [51].

$$R^2 = 1 - \left(\frac{\sum_{i=1}^{N} \left(t_i - o_i\right)^2}{\sum_{i=1}^{N} o_i^2} \right) \quad (6)$$

$$\text{RMSE} = \left(\frac{\sum_{i=1}^{N} \left|t_i - o_i\right|^2}{N} \right)^{1/2} \quad (7)$$

$$\text{MAPE} = \frac{1}{N} \sum_{i=1}^{N} \left(\left| \frac{t_i - o_i}{o_i} \right| \right) \quad (8)$$

Comparisons of the actual T and Fr results obtained after the experiments and the training and test results obtained by regression analysis are given in Figs. 12, 13, 14 and 15. It can be clearly seen from the figures that the predictions of the developed models are quite near to the actual experimental results. This indicates that the created regression equations will be effective for the prediction of T and Fr values.

In addition, the accuracy of the regression model was checked with R^2 and RMSE values. These statistical analysis values for T and Fr are given in Table 5. For the cutting zone temperature prediction in the regression model, R^2 in the test data was calculated as 0.994042 and 0.988224 for dry and RHVT machining, respectively. Test for resultant cutting

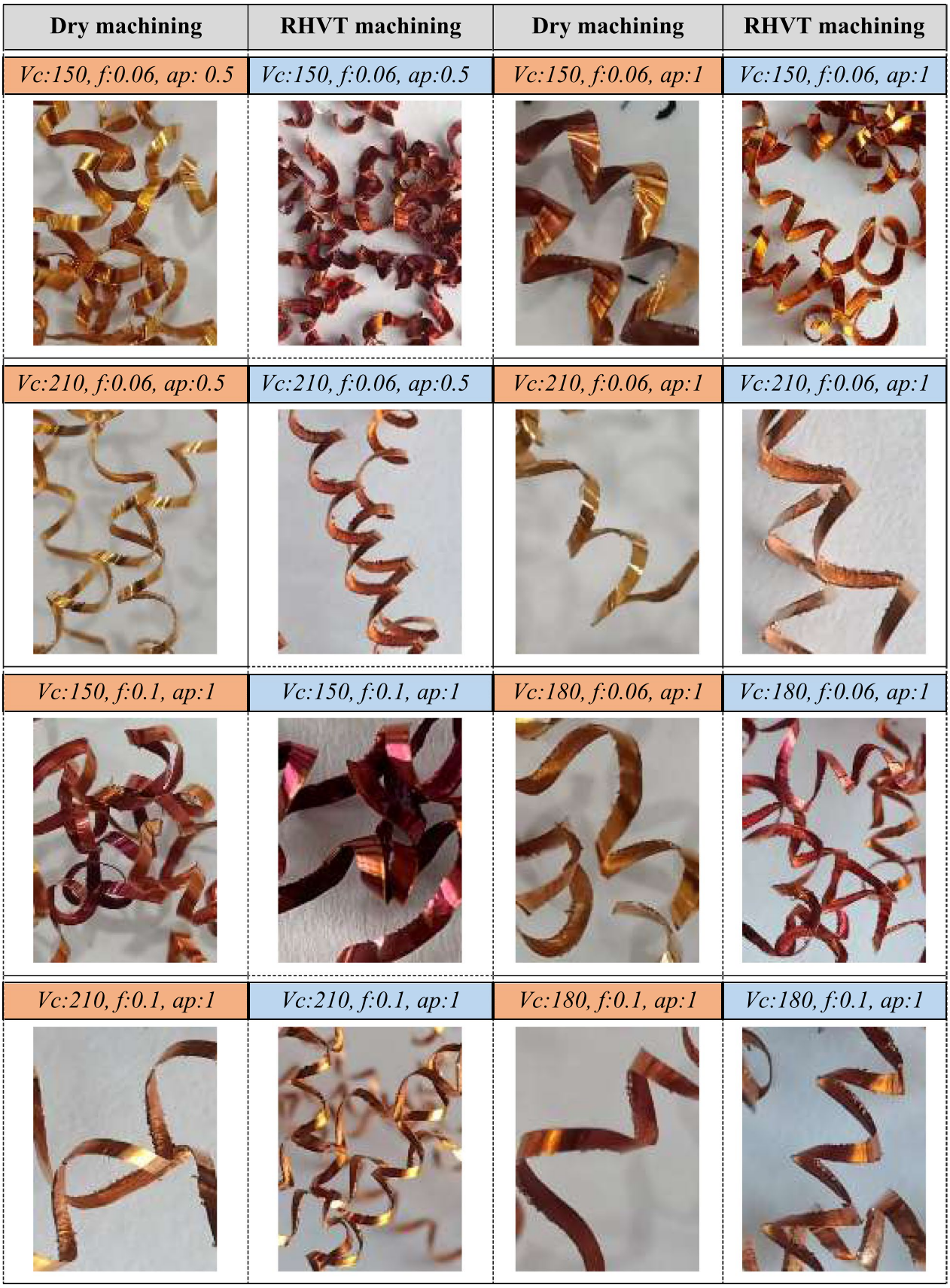

Fig. 11 Chip morphology to the cutting environments and parameters (100X)

force the R^2 value of the results was determined as 0.996399 in the dry condition and 0.989649 in the RHVT condition. As can be seen from the graphs, the developed models fitted the data well. In conclusion, the empirical equation results from regression analysis showed well assent with the experimental results.

4 Conclusion and recommendations

In this study, a comprehensive research was conducted on the modeling of C17500 BeCu alloy turning with the analysis of T, Fr and chip morphology in the changing of cutting parameters in dry and vortex tube cooling environments to contribute to environmentally friendly and sustainable production. The findings are summarized below:

- While the average of the temperatures obtained in the turning by the dry environment was determined as 513 °C, the average temperature in the cutting processes with RHVT cooling was determined as 321 °C. By using RHVT cooling, the cutting zone temperature can be reduced by approximately 62.6% compared with dry machining.
- The lowest cutting zone temperature with by using RHVT was 216 °C with $Vc = 150$ m/min, $f = 0.1$ mm/rev, and $ap = 1$ mm. Considering that tool wear increases at high cutting temperature, this result indicates that tool life will be longer in machining with RHVT application.

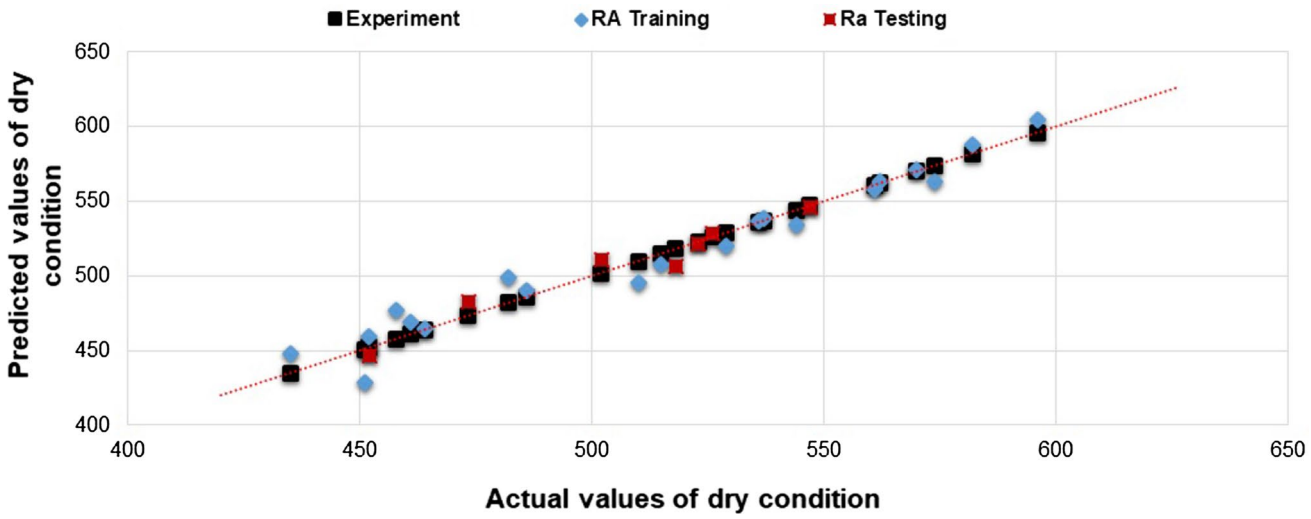

Fig. 12 Comparison of cutting zone temperature results for dry condition

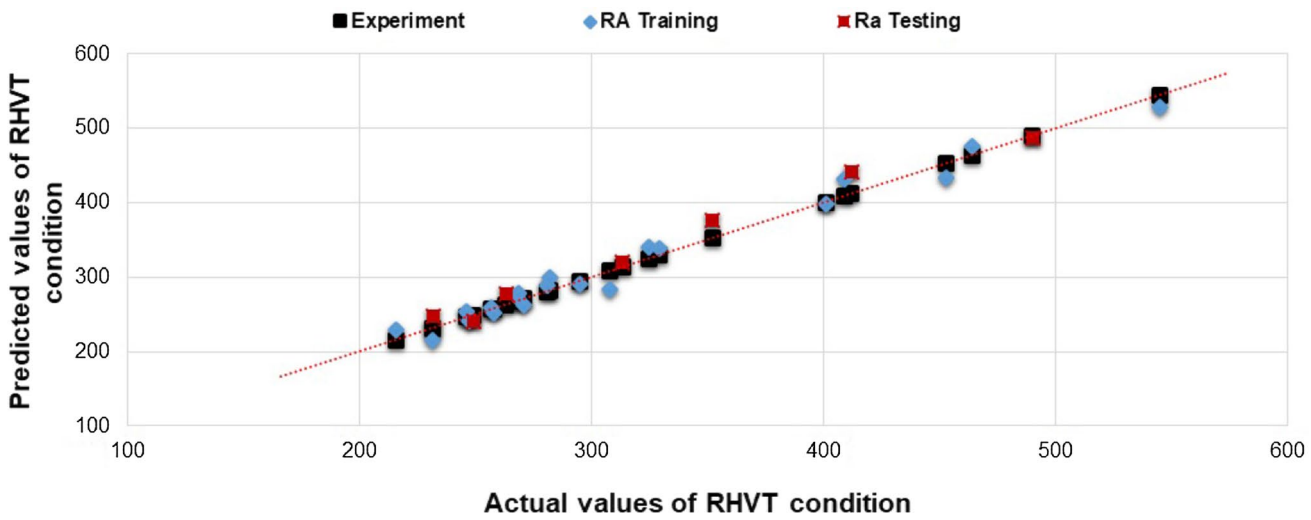

Fig. 13 Comparison of cutting zone temperature for RHVT condition

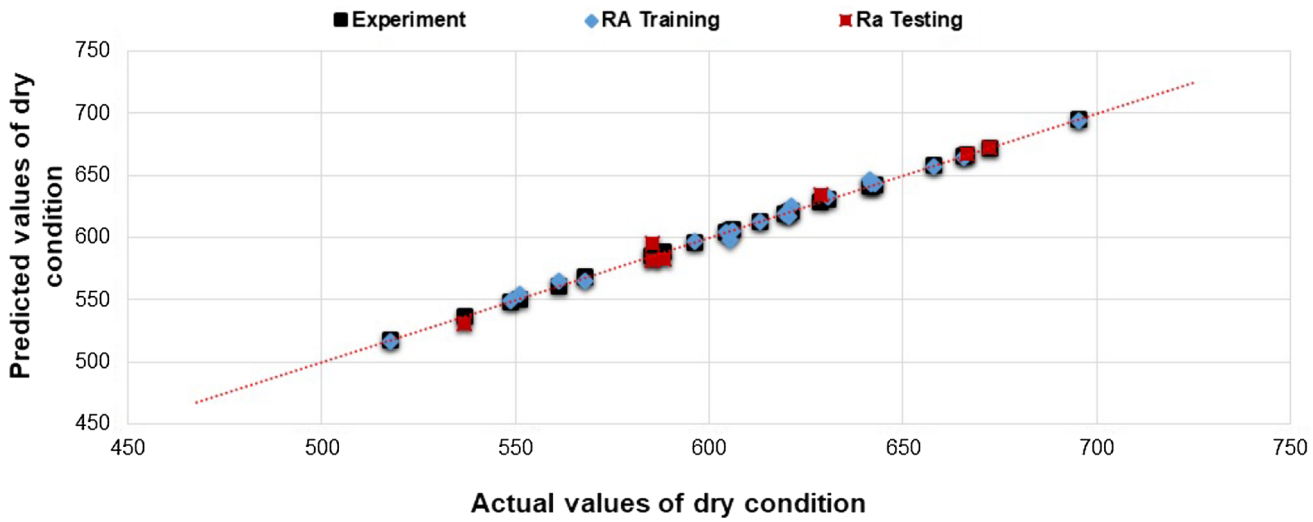

Fig. 14 Comparison of resultant cutting force for dry condition

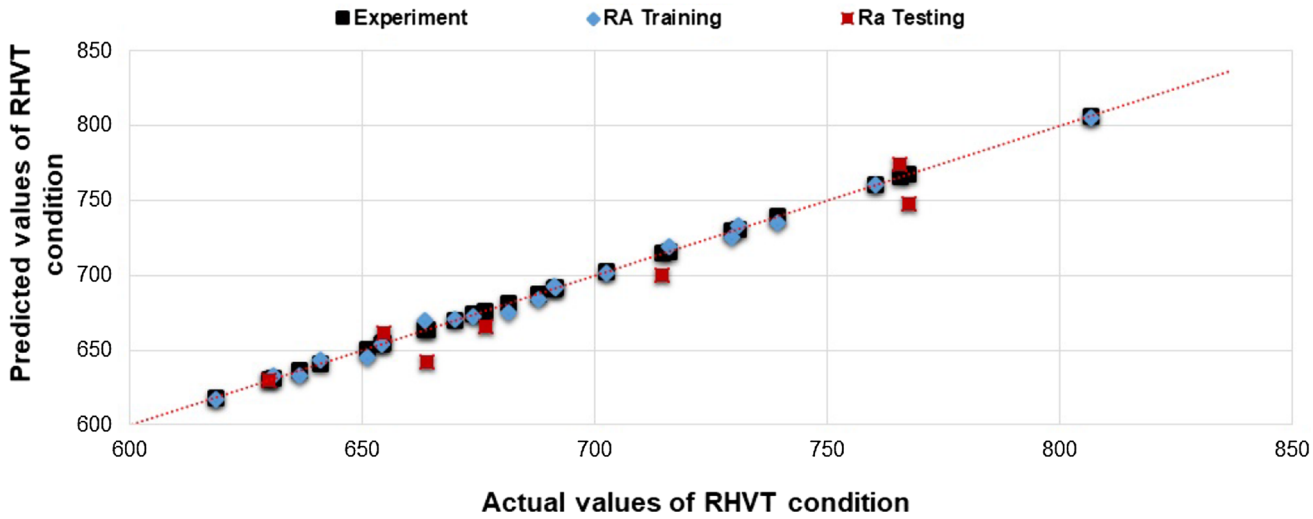

Fig. 15 Comparison of resultant cutting force for RHVT condition

Table 5 Statistical results for cutting zone temperature

	R^2 training	R^2 testing	RMSE training	RMSE testing
$T_{(Dry)}$	0.985921	0.994042	0.115415	0.084763
$T_{(RHVT)}$	0.995796	0.988224	0.079403	0.134083
$Fr_{(Dry)}$	0.998968	0.996399	0.028749	0.061626
$Fr_{(RHVT)}$	0.999355	0.989649	0.028714	0.128138

- While the lowest Fr force was measured as 517.6 N in the dry machining with $Vc = 210$ m/min, $f = 0.06$ mm/rev, $ap = 5$ mm, the highest Fr force was measured as 806.6 N in the RHVT condition with $Vc = 150$ m/min, $f = 0.1$ mm/rev, $ap = 1$ mm.
- The average Fr values obtained in the cutting processes under RHVT conditions were approximately 11.6% higher than the average values of the dry cutting condition. This result was caused by the change of the tool geometry due to BUL and BUE formed on the cutting edges and side surfaces of the cutting tool.
- Chip morphology according to the cutting environment was examined, although shorter and curved chips are usually produced in RHVT; larger CTR values are achieved. These results indicate that the machined surfaces will be formed in a smoother structure with RHVT application and tool deformations due to chip wrapping can be prevented.
- The R^2 values of the predictive models obtained by regression analysis for T and Fr are very close to 1, indi-

cating that the models can be used safely in similar applications.

- In the future, research on energy consumption and surface quality can be carried out to contribute to sustainability by using both environmentally friendly and cost-effective cutting media for this and similar materials.

Declarations

Conflict of interest The author declares that he has no known competing financial interests or personal relationships that could have appeared to influence the work reported in this paper.

References

1. Sharma A, Datta D, Balasubramaniam R (2018) An investigation of tool and hard particle interaction in nanoscale cutting of copper beryllium. Comput Mater Sci 145:208–223. https://doi.org/10.1016/j.commatsci.2018.01.011
2. Alagarsamy SV, Ravichandran M, Meignanamoorthy M et al (2020) Influence of CNC turning variables on high strength Beryllium-Copper (C17200) alloy using tungsten carbide insert. Mater Today Proc 27:925–930. https://doi.org/10.1016/j.matpr.2020.01.260
3. Zuo J, Lin Y, Zheng J et al (2019) An investigation of thermal-mechanical interaction effect on PVD coated tool wear for milling Be/Cu alloy. Vacuum 167:271–279. https://doi.org/10.1016/j.vacuum.2019.06.017
4. Santos MD, Fukumasu NK, Tschiptschin AP et al (2022) Effect of Ti/Si and Ti/TiN/Si interlayers on the structure, properties, and tribological behavior of an a-C film deposited onto a C17200 copper-beryllium alloy. Surf Coat Technol 441:128561. https://doi.org/10.1016/j.surfcoat.2022.128561
5. García-Martínez E, Miguel V, Manjabacas MC et al (2021) Low initial lubrication procedure in the machining of copper-nickel 70/30 ASTM B122 alloy. J Manuf Process 62:623–631. https://doi.org/10.1016/j.jmapro.2021.01.002
6. Huang P, Li H, Zhu W-L et al (2020) Effects of eco-friendly cooling strategy on machining performance in micro-scale diamond turning of Ti–6Al–4V. J Clean Prod 243:118526. https://doi.org/10.1016/j.jclepro.2019.118526
7. Singh D, Venkateswara Rao P (2007) Optimization of tool geometry and cutting parameters for hard turning. Mater Manuf Process 22:15–21. https://doi.org/10.1080/10426910601015816
8. Gupta A, Ramagopal S, Batish A, Bhattacharya A (2014) Surface roughness and profile error in precision diamond turning of C18000. Mater Manuf Process 29:606–613. https://doi.org/10.1080/10426914.2014.901529
9. Saikiran M, kumar P, (2019) An investigation on the effects of vegetable oil based cutting fluids in the machining of copper alloys. Mater Today Proc 19:455–461. https://doi.org/10.1016/j.matpr.2019.07.635
10. Hong SY, Ding Y, Jeong J (2002) Experimental evaluation of friction coefficient and liquid nitrogen lubrication effect in cryogenic machining. Mach Sci Technol 6:235–250. https://doi.org/10.1081/MST-120005958
11. Sharma AK, Tiwari AK, Dixit AR (2016) Effects of Minimum Quantity Lubrication (MQL) in machining processes using conventional and nanofluid based cutting fluids: a comprehensive review. J Clean Prod 127:1–18. https://doi.org/10.1016/j.jclepro.2016.03.146
12. Yıldırım ÇV, Sarıkaya M, Kıvak T, Şirin Ş (2019) The effect of addition of hBN nanoparticles to nanofluid-MQL on tool wear patterns, tool life, roughness and temperature in turning of Ni-based Inconel 625. Tribol Int 134:443–456. https://doi.org/10.1016/j.triboint.2019.02.027
13. Kumar Gajrani K, Ravi Sankar M (2017) Past and current status of eco-friendly vegetable oil based metal cutting fluids. Mater Today Proc 4:3786–3795. https://doi.org/10.1016/j.matpr.2017.02.275
14. Katna R, Suhaib M, Agrawal N (2020) Nonedible vegetable oil-based cutting fluids for machining processes—a review. Mater Manuf Process 35:1–32. https://doi.org/10.1080/10426914.2019.1697446
15. Su Y, Gong L, Li B et al (2016) Performance evaluation of nanofluid MQL with vegetable-based oil and ester oil as base fluids in turning. Int J Adv Manuf Technol 83:2083–2089. https://doi.org/10.1007/s00170-015-7730-x
16. Nguyen TK, Do I, Kwon P (2012) A tribological study of vegetable oil enhanced by nano-platelets and implication in MQL machining. Int J Precis Eng Manuf 13:1077–1083. https://doi.org/10.1007/s12541-012-0141-0
17. Gürkan D, Yaşar SA, Uzun G, Korkut İ (2020) Vorteks soğutma yönteminin talaşlı imalat yöntemleri ve kesme parametrelerine göre incelenmesi. Gazi Univ J Sci Part C Des Technol 8:730–745. https://doi.org/10.29109/gujsc.727746
18. Çakıroğlu R (2021) Machinability analysis of Inconel 718 superalloy with AlTiN-coated carbide tool under different cutting environments. Arab J Sci Eng 46:8055–8073. https://doi.org/10.1007/s13369-021-05626-3
19. Çakır O, Kıyak M, Altan E (2004) Comparison of gases applications to wet and dry cuttings in turning. J Mater Process Technol 153–154:35–41. https://doi.org/10.1016/j.jmatprotec.2004.04.190
20. Rubio EM, Agustina B, Marín M, Bericua A (2015) Cooling systems based on cold compressed air: a review of the applications in machining processes. Procedia Eng 132:413–418. https://doi.org/10.1016/j.proeng.2015.12.513
21. Ko TJ, Kim HS, Chung BG (1999) Air-oil cooling method for turning of hardened material. Int J Adv Manuf Technol 15:470–477. https://doi.org/10.1007/s001700050091
22. Hu JS, Liu DX, Liu YZ et al (2008) Experimental investigation on air cooling of GCr15. Key Eng Mater 375–376:197–200. https://doi.org/10.4028/www.scientific.net/KEM.375-376.197
23. Nelge B, Devade K, Pise AT, Kale VM (2014) Thermal and metallographic investigation for H13A and AISI1050 using vortex tube jet assisted (VTJA) machining, pp 1–7
24. Balki N, Nelge B, Ingle A (2017) Experimental investigation of environment friendly cooling methods for different machining conditions. Int J Eng Sci Res Technol 6:186–191. https://doi.org/10.5281/zenodo.1042116
25. Liu J, Chou YK (2008) Vortex-tube cooling for tool wear reduction in A390 dry machining. American Society of Mechanical Engineers Digital Collection, pp 837–838
26. Mia M, Singh G, Gupta MK, Sharma VS (2018) Influence of Ranque-Hilsch vortex tube and nitrogen gas assisted MQL in precision turning of Al 6061–T6. Precis Eng 53:289–299. https://doi.org/10.1016/j.precisioneng.2018.04.011
27. Kumar S, Gandotra S (2021) Effect of cooling air on machining performance during hard turning. Mater Today Proc 38:2213–2216. https://doi.org/10.1016/j.matpr.2020.06.263
28. Günay M, Korkmaz ME, Yaşar N (2020) Performance analysis of coated carbide tool in turning of Nimonic 80A superalloy under

different cutting environments. J Manuf Process 56:678–687. https://doi.org/10.1016/j.jmapro.2020.05.031
29. Pradeep Kumar KV, Jyothilakshmi R, Hemanth Kumar KJ, Patil S (2022) Wear and surface finish studies on CVD coated tungsten carbide indexable inserts. Mater Today Proc 52:2322–2326. https://doi.org/10.1016/j.matpr.2021.11.431
30. Bülbül AE, Dilipak H, Sarıkaya M, Yılmaz V (2016) Optimization of the wear behavior of uncoated, TiN and AlTiN coated cold work tool steel 1.2379 using response surface methodology. Mater Test 58:12–19. https://doi.org/10.3139/120.110803
31. Kirmaci V, Kaya H, Cebeci I (2018) An experimental and exergy analysis of a thermal performance of a counter flow Ranque-Hilsch vortex tube with different nozzle materials. Int J Refrig 85:240–254. https://doi.org/10.1016/j.ijrefrig.2017.10.003
32. Dhar NR, Kamruzzaman M (2007) Cutting temperature, tool wear, surface roughness and dimensional deviation in turning AISI-4037 steel under cryogenic condition. Int J Mach Tools Manuf 47:754–759. https://doi.org/10.1016/j.ijmachtools.2006.09.018
33. Abdelnasser E, Barakat A, Elsanabary S et al (2020) Precision hard turning of Ti6Al4V using polycrystalline diamond inserts: surface quality, cutting temperature and productivity in conventional and high-speed machining. Materials 13:5677. https://doi.org/10.3390/ma13245677
34. Khan A, Maity K (2017) Comparative study of some machinability aspects in turning of pure titanium with untreated and cryogenically treated carbide inserts. J Manuf Process 28:272–284. https://doi.org/10.1016/j.jmapro.2017.05.018
35. Rezende BA, Magalhães F de C, Campos Rubio JC (2020) Study of the measurement and mathematical modelling of temperature in turning by means equivalent thermal conductivity. Measurement 152:107275. https://doi.org/10.1016/j.measurement.2019.107275
36. Taha Z, Salaam HA, Ya TMYST et al (2013) Vortex tube air cooling: the effect on surface roughness and power consumption in dry turning. Int J Automot Mech Eng 8:1477–1586. https://doi.org/10.15282/ijame.8.2013.34.0122
37. Kalyon A, Günay M, Özyürek D (2018) Application of grey relational analysis based on Taguchi method for optimizing machining parameters in hard turning of high chrome cast iron. Adv Manuf 6:419–429. https://doi.org/10.1007/s40436-018-0231-z
38. Kaçal A (2020) Effect of machining parameters on turning of Inconel X750 using PVD coated carbide inserts. JSIR Vol7903 March 2020
39. Shahabi HH, Ratnam MM (2010) In-cycle detection of built-up edge (BUE) from 2-D images of cutting tools using machine vision. Int J Adv Manuf Technol 46:1179–1189
40. Gómez-Parra A, Álvarez-Alcón M, Salguero J et al (2013) Analysis of the evolution of the Built-Up Edge and Built-Up Layer formation mechanisms in the dry turning of aeronautical aluminium alloys. Wear 302:1209–1218. https://doi.org/10.1016/j.wear.2012.12.001
41. Carrilero MS, Bienvenido R, Sánchez JM et al (2002) A SEM and EDS insight into the BUL and BUE differences in the turning processes of AA2024 Al–Cu alloy. Int J Mach Tools Manuf 42:215–220. https://doi.org/10.1016/S0890-6955(01)00112-2
42. Trujillo FJ, Sevilla L, Marcos M (2017) Experimental parametric model for indirect adhesion wear measurement in the dry turning of UNS A97075 (Al-Zn) alloy. Materials 10:152. https://doi.org/10.3390/ma10020152
43. Nobel C, Hofmann U, Klocke F, Veselovac D (2016) Experimental investigation of chip formation, flow, and breakage in free orthogonal cutting of copper-zinc alloys. Int J Adv Manuf Technol 5–8:1127–1140. https://doi.org/10.1007/s00170-015-7749-z
44. Pawade RS, Joshi SS (2011) Mechanism of chip formation in high-speed turning of inconel 718. Mach Sci Technol 15:132–152. https://doi.org/10.1080/10910344.2011.557974
45. Islam S, Khandoker N, Izham M et al (2017) Development of a low cost MQL setup for turning operations. MATEC Web Conf 95:10004. https://doi.org/10.1051/matecconf/20179510004
46. Tamizharasan T, Senthilkumar N, Selvakumar V, Dinesh S (2019) Taguchi's methodology of optimizing turning parameters over chip thickness ratio in machining P/M AMMC. SN Appl Sci 1:160. https://doi.org/10.1007/s42452-019-0170-8
47. Yilmaz V, Sarikaya M, Dilipak H (2015) Deep micro-hole drilling for hadfield steel by electro-discharge machining (EDM). Mater Tehnol. https://doi.org/10.17222/mit.2014.091
48. Yaşar N, Günay M (2019) Experimental investigation on novel drilling strategy of CFRP laminates using variable feed rate. J Braz Soc Mech Sci Eng 41:150. https://doi.org/10.1007/s40430-019-1658-2
49. Günay M, Meral T (2020) Modelling and multiresponse optimization for minimizing burr height, thrust force and surface roughness in drilling of ferritic stainless steel. Sādhanā 45:273. https://doi.org/10.1007/s12046-020-01490-3
50. Şahîn İ (2014) Yapay Sinir Ağları İle Al/Sic Kompozit Malzemenin Yüzey Pürüzlülüğünün Tahmini. Gazi Üniversitesi Mühendis Mimar Fakültesi Derg. https://doi.org/10.17341/gummfd.82690
51. Hanief M, Wani MF, Charoo MS (2017) Modeling and prediction of cutting forces during the turning of red brass (C23000) using ANN and regression analysis. Eng Sci Technol Int J 20:1220–1226. https://doi.org/10.1016/j.jestch.2016.10.019

Publisher's Note Springer Nature remains neutral with regard to jurisdictional claims in published maps and institutional affiliations.

Springer Nature or its licensor holds exclusive rights to this article under a publishing agreement with the author(s) or other rightsholder(s); author self-archiving of the accepted manuscript version of this article is solely governed by the terms of such publishing agreement and applicable law.